# Supplementary Information

## THz enantiomers of drugs recognized by the polarization enhancement of gold nanoparticles on the asymmetric metasurface

Wei-Nan Shi[a], Yi-Ming Wang,[a] Fei Fan[a, b, *], Jia-Yue Liu,[a] Jie-Rong Cheng, [a] Xiang-Hui Wang[a, **], Sheng-Jiang Chang[a, b]

[a] *Institute of Modern Optics, Nankai University, Tianjin Key Laboratory of Micro-scale Optical Information Science and Technology, Tianjin 300350, China.*

[b] *Tianjin Key Laboratory of Optoelectronic Sensor and Sensing Network Technology, Tianjin 300350, China.*

*Corresponding authors: fanfei@nankai.edu.cn (Fei Fan);

wangxianghui@nankai.edu.cn (Xianghui Wang)

## S1. Data processing methods in the THz experiment

The detection accuracy of polarization characteristic parameters in the system mainly depends on the polarization angle resolution of the system, which is mainly determined by the polarization degree ($R_p$) and minimum polarization angle ($M_{PA}$)of the system, which can be calculated by:

$$R_P = 20 \times \log\left(\frac{A_{\parallel} - A_{\perp}}{A_{\parallel} + A_{\perp}}\right)$$
$$M_{PA} = \arctan\left(\frac{A_{\perp}^2}{A_{\parallel}^2}\right) \quad (1)$$

here $A_{\parallel}$ and $A_{\perp}$ is the amplitude transmittance when the directions of the two polarizers are parallel and orthogonal. The higher the polarization degree of the polarizer, the lower the signal-to-noise ratio of the system, the smaller the value of $M_{PA}$, and the higher the angular resolution of the system. Therefore, it depends on the performance of the system itself. The measurement results of the sensing accuracy of our self-built system are shown in Figure S1. Within the range of 0.2~0.8 THz, $D_p$ is lower than -36 dB, and $M_{PA}$ is less than 0.01°.

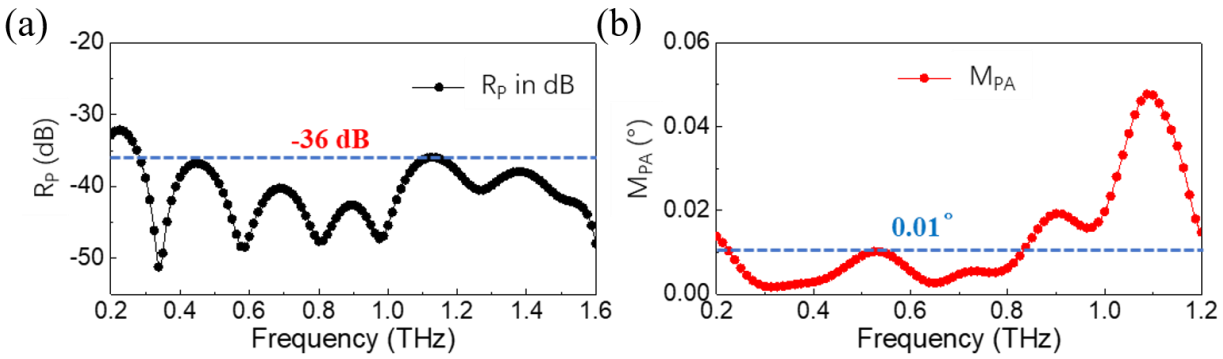


**Fig. S1.** (a) $R_p$ spectra and (b) $M_{PA}$ spectra of our system.

The calculation method of polarization parameters is as follows: through experimental measurement, the amplitude and phase reflection spectra in two orthogonal directions can be obtained after the Fourier transform of the THz time-domain signal: $A_{x,y}(\omega)$ and $\phi_{x,y}(\omega)$.

Through calculation, the complete polarization state of the detected signal can be reconstructed, expressed as:

$$\left(\frac{E_x}{A_x}\right)^2+\left(\frac{E_y}{A_y}\right)^2-\frac{2E_xE_y}{A_xA_y}\cos\Delta\phi=\sin^2\Delta\phi \tag{2}$$

where $E_x$ and $E_y$ denote the $x$ and $y$ components of the electric field vector $\boldsymbol{E}$ of the detection signal, respectively, and $\Delta\phi=\phi_x-\phi_y$. As shown in Fig. S2(a), when the incident wave is a 45° polarized linearly wave, after passing through the metasurface, the reflected wave is elliptically polarized, the left circular polarized (LCP) and right circular polarized (RCP) components can also be calculated by:

$$\begin{aligned}R_{LCP}(\omega)&=\frac{1}{2}\left(A_x(\omega)e^{i\phi_x(\omega)}-iA_y(\omega)e^{i\phi_y(\omega)}\right)\\R_{RCP}(\omega)&=\frac{1}{2}\left(A_x(\omega)e^{i\phi_x(\omega)}+iA_y(\omega)e^{i\phi_y(\omega)}\right)\end{aligned} \tag{3}$$

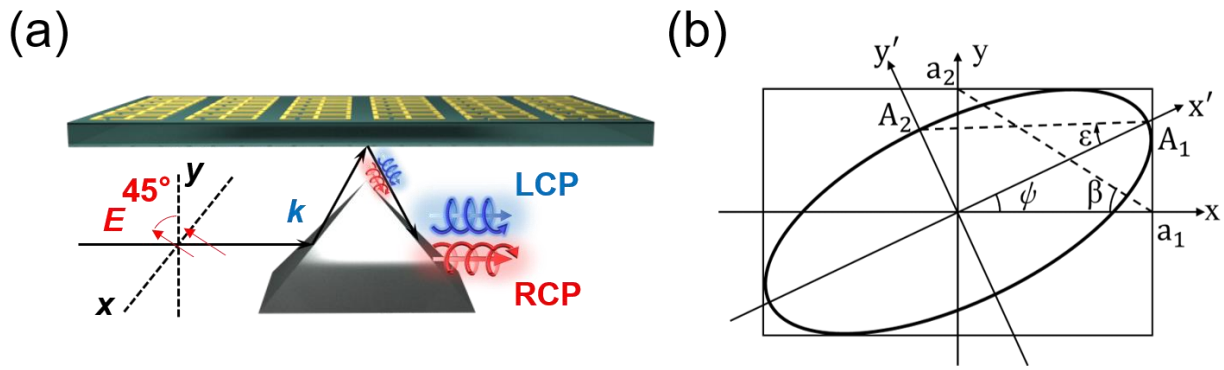


**Fig. S2**. (a) Schematic diagram of polarization conversion and chirality in metasurface sensor; (b) Geometry and physical parameters in polarization ellipse of electric field vector.

In addition, as shown in Fig. S2(b), two polarization parameters, polarization ellipsoid angle (PEA, denoted by $\varepsilon$), which is determined by the ratio of the LCP and RCP components. And polarization rotation angle (PRA, denoted by $\psi$), which is determined by the phase difference

between the LCP and RCP components, are used to characterize the polarization state conversions in the spectral domain:

$$\begin{aligned} \sin 2\varepsilon(\omega) &= \sin 2\beta(\omega)\sin\Delta\phi(\omega) \\ \tan 2\psi(\omega) &= \tan 2\beta(\omega)\cos\Delta\phi(\omega) \end{aligned} \tag{4}$$

here, $\tan\beta = A_x / A_y$, PEA is used to describe the ellipticity of the polarization state of the output light, with positive and negative values reflecting the chirality of the output light, positive values representing RCP, and negative values representing LCP, ranging from -45° to +45°, 0° corresponds to linear polarization and ±45° corresponds to circular polarization. PRA describes the rotation angle in the polarization direction of the output light, which ranges from -90° to +90°, positive values correspond to clockwise directions and negative values correspond to counterclockwise directions.

If the incident wave is circularly polarized, it is necessary to detect a pair of orthogonal components of the incident wave and the output wave simultaneously. In our experiment, by rotating the polarizer, the incident wave is incident at +45° and -45°, respectively. Then the components in different directions can also be detected, and the reflection spectrum of the metasurface can be obtained by:

$$\begin{aligned} R_{rr} &= \frac{1}{2}\left[ (R_{45^\circ,45^\circ} + R_{-45^\circ,-45^\circ}) + i(R_{45^\circ,-45^\circ} - R_{-45^\circ,45^\circ}) \right] \\ R_{ll} &= \frac{1}{2}\left[ (R_{45^\circ,45^\circ} + R_{-45^\circ,-45^\circ}) - i(R_{45^\circ,-45^\circ} - R_{-45^\circ,45^\circ}) \right] \end{aligned} \tag{5}$$

Among them, "*r*" and "*l*" represent RCP and LCP components, $R_{rr}$ denotes RCP incident and RCP reflect, $R_{ll}$ denotes LCP incident and LCP reflect. "45°" and "-45°" represent linear polarization components in the direction of 45° and -45°, the first quantity of the lower angle mark represents

the direction of the output polarization state, and the second represents the direction of the incident polarization state. Circular dichroism (*CD*) spectrum is calculated as follows:

$$CD(\omega)=20\times\log_{10}\left(\frac{R_{ll}(\omega)}{R_{rr}(\omega)}\right) \tag{6}$$

which represents the difference in reflection amplitude between LCP and RCP wave.

## S2. Molecular structure of different chiral drugs

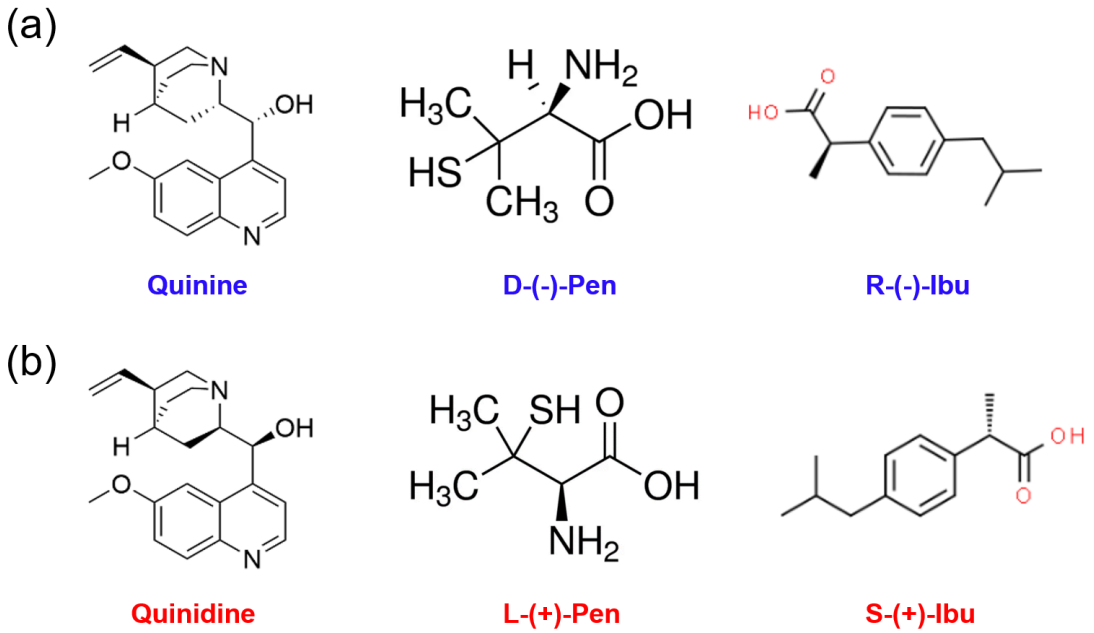


**Fig. S3.** Molecular structure of (a) left-handed enantiomers and (b) right-handed enantiomers.

Fig. S3a are the left-handed drugs used in our experiment and Fig. S3b shows the corresponding right-handed enantiomers. Here, "+" and "-" represent the optical activity of the sample, "-" represents left-handed rotation, and "+" is right-handed rotation. As can be seen from the figure, these samples are composed of the same molecules, but the spatial structure of the molecules is different. All sample names are simplified in the manuscript, such as writing "D-(-)-Pen" as "D-Pen".

## S3. Electric field distribution

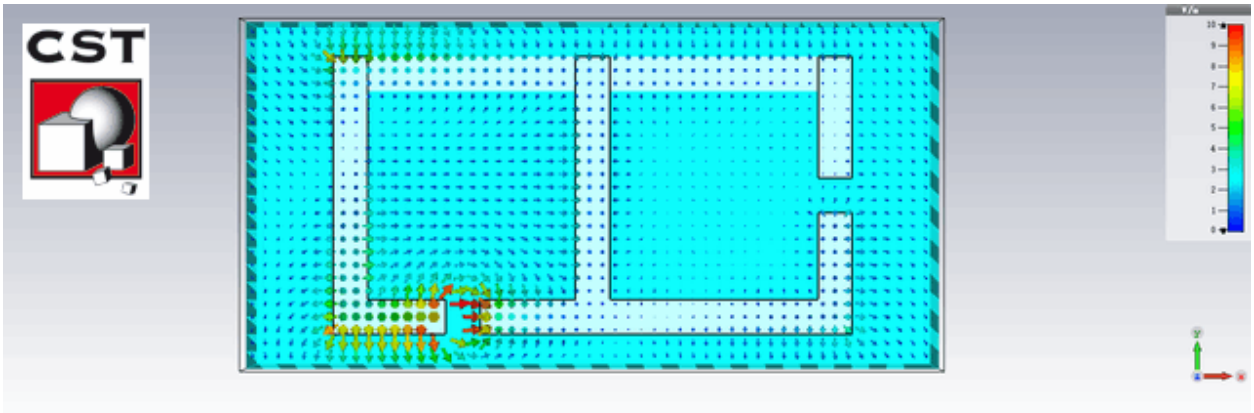


**Fig. S4.** Surface electric field vector distribution at 0.45 THz in *xy*-plane of the metasurface.

The electric field flows in the left and right metal rings of the unit cell are different: in the left ring, with the phase change, the electric field vectors converge from the left to the right of the opening, forming a left-to-right electric field distribution; while in the right ring, the electric field vector flows from below the opening to above, forming a bottom-to-top electric field distribution. This asymmetric electric field distribution makes the metasurface acquire a strong chirality response (the dynamic distribution of the electric field is shown in Video S1).

## S4. Chiral characterization of the metasurface

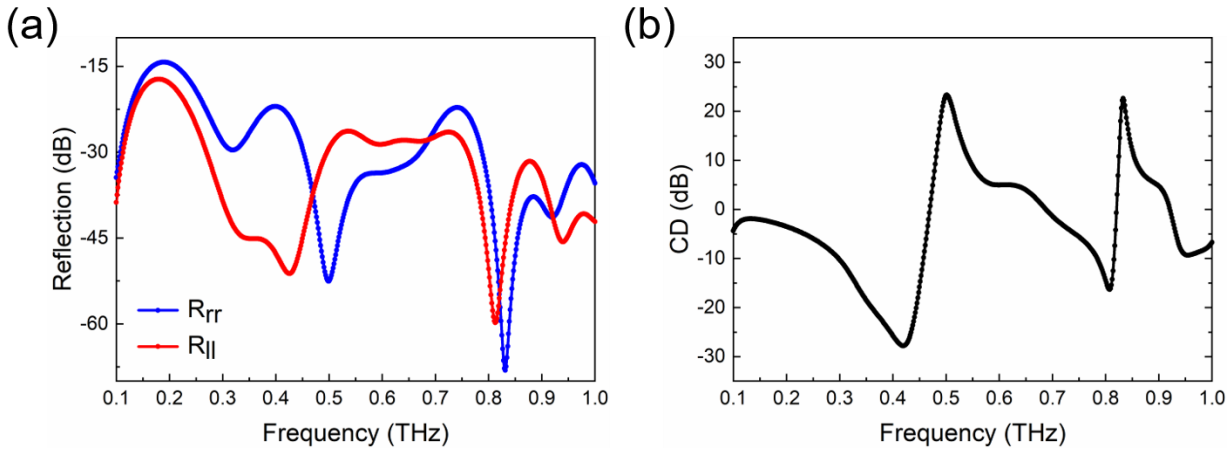


**Fig. S5.** (a) Reflection of LCP and RCP spectra of the metasurface. (b) Circular dichroism (CD) spectra of the metasurface.

When the THz wave is normal incidence to the metasurface, the metasurface is achiral, so in our experiment, we make the THz wave incident to the metasurface with an angle of 30°, the metal pattern on the metasurface breaks the rotational symmetry, and it is possible to produce chirality when the THz wave oblique incident to it. To prove our point, we experimentally measured the *CD* of the metasurface excited by circularly polarized waves at oblique incidence.

According to Equations (5) and (6) in S1, we calculated the $R_{rr}$ , $R_{ll,}$ and *CD* of the metasurface, as shown in Fig. S5. From the figures, it can be observed that the metasurface can produce a strong *CD* in the ranges of 0.4~0.55 THz and 0.75~0.85 THz, among them, the *CD* of -30dB at 0.42 THz is the strongest, so in the sensing experiments, we mainly investigate the sensing performance of the metasurface in the range of 0.4-0.55THz.

## S5. PRA and RCP spectra for Quinidine and Quinine

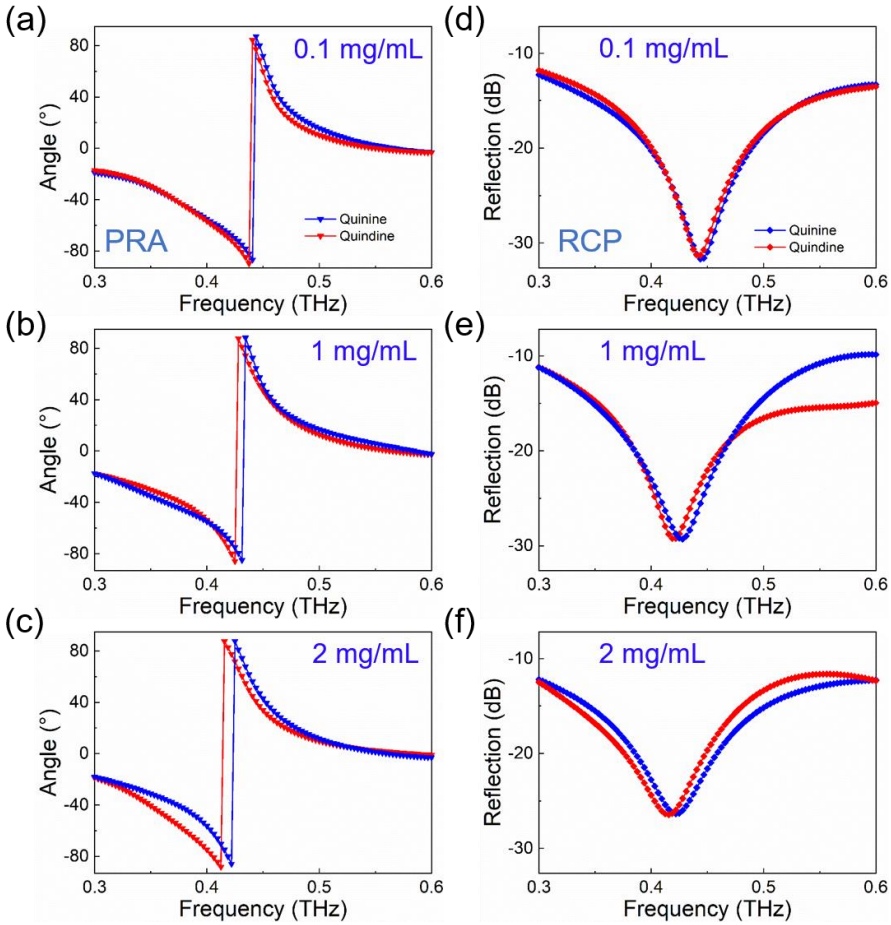


**Fig. S6.** PRA spectra for Quinine and Quinidine at the concentration of (a) 0.1 mg/ml (b) 1 mg/ml and (c) 2 mg/ml. RCP spectra for Quinine and Quinidine at the concentration of (d) 0.1 mg/ml (e) 1 mg/ml and (f) 2 mg/ml.

Figs. S6 shows the reflection spectra of PRA and RCP. The difference between enantiomers is mainly reflected in the frequency position of the spectral peak, the frequency shift of Quinidine (right-handed enantiomer) in different concentrations is always greater than Quinine (left-handed enantiomer). At low concentrations, the difference between enantiomers is only 2-3 GHz, and with the increase of concentration, the difference in frequency shift becomes more obvious, the frequency difference is about 10 GHz at 2 mg/mL.

## S6. PEA spectra for Pen and Ibu

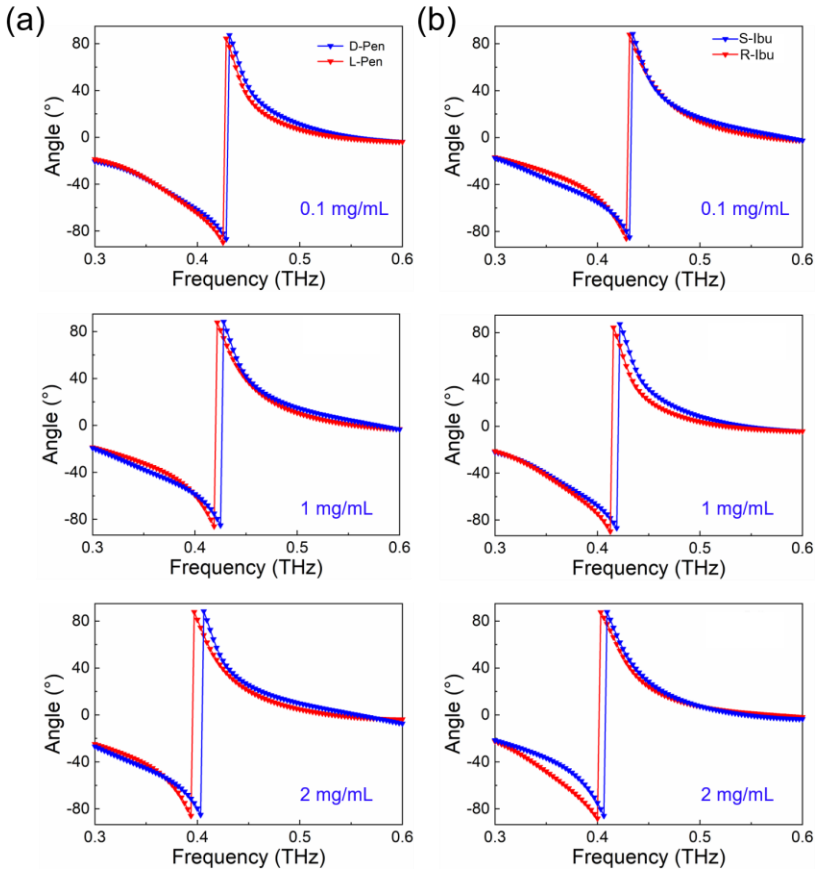


**Fig. S7.** The measured PRA spectra for (a)Pen and (b) Ibu at different concentrations.

Figs. S7 shows the reflection spectra of PRA for Pen and Ibu at different concentrations. As can be seen from the figure, for different enantiomers, the distinguishing ability of the PRA spectrum is limited because the value of PRA is determined by the phase difference between the LCP and RCP components of the output wave, and the difference in phase delay caused by enantiomers is not obvious. Therefore, in our work, the identification of enantiomers is mainly achieved by PEA spectra.